Giant Acceleration of Diffusion Observed in a Single-Molecule Experiment on F_1-ATPase

Ryunosuke Hayashi,[1] Kazuo Sasaki,[1] Shuichi Nakamura,[1] Seishi Kudo,[1] Yuichi Inoue,[2] Hiroyuki Noji,[3] and Kumiko Hayashi[1,*]

[1]*Department of Applied Physics, School of Engineering, Tohoku University, Sendai 980-8579, Japan*
[2]*Institute of Multidisciplinary Research for Advanced Material, Tohoku University, Sendai 980-8577, Japan*
[3]*Department of Applied Chemistry, School of Engineering, the University of Tokyo, Tokyo 113-8654, Japan*

(Received 26 November 2014; published 16 June 2015)

The giant acceleration (GA) of diffusion is a universal phenomenon predicted by the theoretical analysis given by Reimann *et al.* [Phys. Rev. Lett. 87, 010602 (2001)]. Here we apply the theory of the GA of diffusion to a single-molecule experiment on a rotary motor protein, F_1, which is a component of F_oF_1 adenosine triphosphate synthase. We discuss the energetic properties of F_1 and identify a high energy barrier of the rotary potential to be $20k_BT$, with the condition that the adenosine diphosphates are tightly bound to the F_1 catalytic sites. To conclude, the GA of diffusion is useful for measuring energy barriers in nonequilibrium and single-molecule experiments.

DOI: 10.1103/PhysRevLett.114.248101 PACS numbers: 87.15.-v

The diffusion phenomena of microscopic particles, heat energy, electrons, etc., are common mechanisms that are routinely observed. They occur in solids, liquids, gases, and even in supercritical fluids, as a result of the thermal motion of the atoms and molecules which constitute these media. Many diffusion theories exist in the field of nonequilibrium statistical mechanics, one of which is the giant acceleration (GA) of diffusion [1–3]. According to Ref. [1], when a constant force is applied to a colloidal particle in a periodic potential, the diffusion of the particle is greatly enhanced. An increase of up to 14 orders of magnitude can occur, compared to free thermal diffusion for a realistic experimental setup. The diffusion coefficient as a function of an applied force exhibits a resonance peak at the force value near the critical tilt of the potential, which becomes increasingly pronounced as the environmental temperature decreases or as the energy barrier of the periodic potential rises [Figs. 1(a) and 1(b)]. Previously, giant enhancement of the free thermal diffusion has been observed in experiments on nanoparticles in a force field of Refs. [4,5]. Theoretical and experimental investigations on this issue have developed greatly in recent years [6,7].

In this paper, we present an effective application of the GA of diffusion to a single-molecule experiment on a rotary motor protein, F_1-ATPase (F_1), which is a component of F_oF_1 adenosine triphosphate (ATP) synthase [8]. The minimum complex in F_1 that can act as a motor is the $\alpha_3\beta_3\gamma$ subcomplex [Fig. 2(a)]. When F_1 is isolated from F_o, the γ subunit (the rotor) rotates in the $\alpha_3\beta_3$ subunit (the ring), hydrolyzing ATP into ADP (adenosine diphosphate) and P_i (phosphate). In a cell, F_1 is forced to rotate in the reverse direction by the F_o motor to synthesize ATP from ADP and P_i. In order to enhance the efficiency of the ATP synthesis, F_1 has a mechanism, such as ADP inhibition, to inhibit the ATP hydrolysis caused by the spontaneous rotation of F_1 itself [9]. In fact, we often observe long pauses during a single-molecule assay during which F_1 falls into the ADP inhibition state. At this point, ADP is tightly attached to a catalytic site of F_1 and is not released.

In our study, the application of the GA of diffusion to F_1 made it possible to estimate the high energy barrier of the rotary potential for the first time, under the condition that the ADPs were tightly attached to the catalytic sites of F_1. We forced a rigid F_1 to rotate by applying an external torque using a single-molecule technique [Fig. 2(b)]. We found that the diffusion coefficient of a probe attached to F_1 (as a function of the external torque) shows a resonance peak, which was predicted by the theory of the GA of diffusion. Then the energy barrier of the rotary potential of F_1 was estimated from this peak from the comparison with the theory and found to be approximately $20k_BT$ at 25 °C (where k_B is the Boltzmann constant and T is

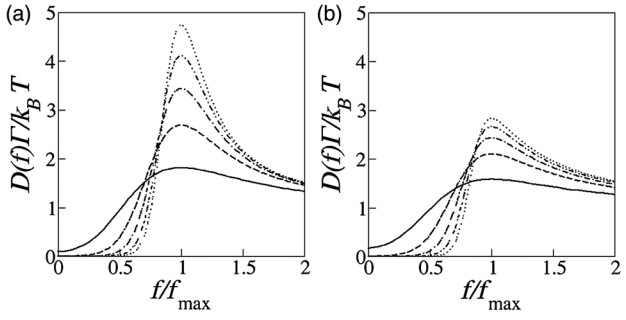

FIG. 1. Theoretical results obtained in Ref. [1] and applied to our F_1 experiments. The dimensionless expression of the diffusion coefficient $D(f)\Gamma/k_BT$ [given in Eq. (3)] as a function of f/f_{max} for (a) a sinusoidal potential [as in Eq. (4)] and for (b) a triangle potential [given in Eq. (5)] with $\Delta_E = 5$, 10, 15, 20, and $25k_BT$ (from bottom to top). Here f_{max} is the force at which $D(f)$ reaches its peak.

the environmental temperature). Finally, we decreased the environmental temperature to 9 °C, and the shift of the energy barrier at 9 °C from that at 25 °C was investigated.

Theory.—We first introduce the theory of the GA of diffusion as discussed in Ref. [1], which was applied to our single-molecule experiment on F_1-ATPase (see the sections below). We consider the one-dimensional model in which a colloidal particle is dragged by a constant external force f, subject to the force exerted by a periodic potential $U(x)$ with a period ℓ, such that

$$\Gamma\frac{dx}{dt} = -\frac{\partial U(x)}{\partial x} + f + \sqrt{2\Gamma k_B T}\xi(t), \tag{1}$$

where $x(t)$ is the particle position, Γ is a friction coefficient, and $\xi(t)$ is Gaussian noise with a variance equal to 1. Then, the diffusion coefficient $D(f)$ is defined as

$$D(f) = \lim_{\Delta t\to\infty} \frac{\langle [x(t+\Delta t) - x(t) - \langle x(t+\Delta t) - x(t)\rangle]^2\rangle}{2\Delta t}, \tag{2}$$

where $\langle\cdots\rangle$ represents the time average in a steady state. For the model given in Eq. (1), $D(f)$ has been calculated [1,2,10] and is expressed as

$$D(f) = \frac{k_B T}{\Gamma}\frac{\frac{1}{\ell}\int_0^\ell dx [I_-(x)]^2 I_+(x)}{\left(\frac{1}{\ell}\int_0^\ell dx I_-(x)\right)^3}, \tag{3}$$

where $I_\pm(x) = \int_0^\ell dy \exp\{[\pm U(x) \mp U(x\mp y) - fy]/k_B T\}$. [Note that the steady state velocity $v(f)$ is expressed in Sec. II of the Supplemental Material [11].]

In Fig. 1(a), $D(f)$ is plotted for a sinusoidal potential

$$U(x) = \frac{\Delta_E}{2}\cos(2\pi x/\ell), \tag{4}$$

and, in Fig. 1(b), for a triangle potential

$$\begin{aligned} U(x) &= \frac{2\Delta_E}{\ell}x - 2n\Delta_E \quad \text{for } n\ell \le x < n\ell + \frac{\ell}{2}, \\ &= -\frac{2\Delta_E}{\ell}x - 2(n+1)\Delta_E \quad \text{for } n\ell + \frac{\ell}{2} \le x < n\ell + \ell, \end{aligned} \tag{5}$$

where $n = 0, \pm 1, \pm 2, \ldots$. $D(f)$ has a peak at $f = f_{\max}$, where $f_{\max}$ is near the critical tilt f_c of $U(x)$ [1,2]. For a sinusoidal potential [Eq. (4)], $D_{\max} \propto \Delta_E^{2/3}$, where $D_{\max} = D(f_{\max})$ when Δ_E becomes large [2]. The divergence of $D_{\max}$ as $\Delta_E \to \infty$ is the GA of diffusion, while $D_{\max}$ shows a convergence for a triangle potential [Eq. (5)] [2]. Thus, the behavior of $D_{\max}$ as a function of Δ_E depends on the functional form of $U(x)$.

Application to single-molecule experiments.—In single-molecule experiments on biomolecules such as DNA, RNA, and proteins, the Boltzmann distribution is often used to measure the potential energy of the system [12]. However, when the energy barrier of a system is too high for molecular diffusion to occur, the distribution cannot be calculated correctly from the measured trajectories. In addition, the observation time in a single-molecule experiment is usually several minutes at most. As well as the theory using a nonequilibrium stationary probability distribution [13], the theory of the GA of diffusion may also be useful in overcoming this common problem in single-molecule experiments; i.e., we can estimate the approximate value of an energy barrier from the diffusion coefficients, under the condition that a molecule is forced to diffuse by applying an external force. For the measured $D(f)$, this theory has several advantages: Eq. (3) is valid for any periodic potential, and the plot of $D(f)\Gamma/k_B T$ vs $f/f_{\max}$ depends only on Δ_E for a particular periodic potential. Note that the mean velocity $v(f)$ can also be used to extract the energetic information of systems, similar to $D(f)$, although the $v(f)$ vs f plot does not exhibit a resonance peak. In fact, we made use of this velocity in the low-temperature experiment conducted on F_1 (Fig. S1 of the Supplemental Material [11]).

In the following section, we demonstrate the GA of diffusion in the single-molecule experiment on the rotary motor protein, F_1-ATPase (F_1). Because the structure of F_1 has a threefold symmetry [Fig. 2(a)], the rotary potential, which is the interaction between the γ subunit and the $\alpha_3\beta_3$ ring, is periodic (with a period of 120°).

F_1 Experiment.—In our single-molecule assay (see Sec. IA of the Supplemental Material [11]), the rotation of the γ subunit was observed as the rotation of a duplex of beads (the diameter of a bead is 460 nm) attached to the γ subunit of F_1 because the size of the γ subunit itself is too small (~2 nm) for its rotation to be observed directly under an optical microscope. (Note that an anisotropically shaped probe such as an actin filament [14] or a bead duplex [15] is useful for detection of the F_1 rotation.) The rotational angle $\theta(t)$ was calculated from the recorded images of the duplex (Fig. 2: right, bottom).

First, we found a bead duplex attached to F_1 in a flow cell with the following conditions: [ATP] = 1 mM and [ADP] = 0 mM, noting that this duplex rotates directionally in the presence of ATP. This means that we did not observe a bead duplex attached to a glass surface through nonspecific interactions but through the F_1 protein itself. After finding the duplex attached to F_1, we exchanged the buffer for one containing [ATP] = 0 mM and [ADP] = 0.5 mM to stop the F_1 rotation. Note that, after the experiment was finished, we again exchanged the buffer for one with [ATP] = 1 mM, [ADP] = 0 mM, to ensure that the F_1 protein we had observed could rotate once more following ATP hydrolysis. Then, we applied an external torque N_{ex} to the bead duplex using the electrorotation method first developed for F_1 in Ref. [16] [Fig. 2(b) and

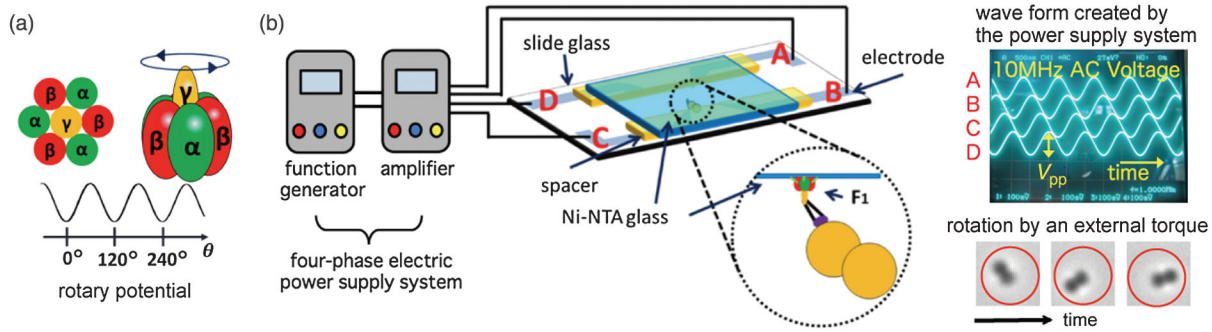

FIG. 2 (color). (a) Because the structure of F_1 has threefold symmetry, its rotary potential has a period of 120°. (b) Electrorotation method. A duplex of polystyrene beads (460-nm diameter), which is a dielectric, is attached to the γ subunit of F_1. F_1 is fixed on the top glass surface (the Ni-NTA-coated coverslip). At the center of the four electrodes, a rotating electric field with a frequency of 10 MHz is generated by applying sinusoidal voltages with a $\pi/2$ phase shift. The phase delay between the electric field and the dielectric moment of the duplex generates a constant torque, N_{ex}.

Sec. IB of the Supplemental Material [11]]. Because the polystyrene bead duplex is a dielectric, it can be rotated by the electrical rotary field. Then, $N_{ex} \propto V_{pp}^2$ [16], where V_{pp} is the peak-to-peak voltage of the applied sinusoidal voltage [Fig. 2(b), right panel]. As V_{pp} was increased, the bead duplex attached to F_1 began to rotate faster and in the same direction as in the ATP hydrolysis case [Fig. 3(a), left panel]. (The positive direction is set to the direction of the F_1 ATP hydrolysis rotation).

As shown in Fig. 3(b) (right panel), we calculated the logarithm of the steady state distribution $P(\theta)$ of θ for $V_{pp} = 14.0$ V, the region in which the mean angular velocity ω is not increased nonlinearly [Fig. 3(b), left panel], in order to infer the functional form of the F_1 rotary potential. (Note that, for $V_{pp} = 0$ V, $P(\theta)$ could not be calculated correctly because the bead duplex did not diffuse significantly, as a result of the high energy barrier of the rotary potential under the high ADP conditions.) Because $-\ln[P(\theta)]$ in the case of $V_{pp} = 14.0$ V seems well described by a symmetric sinusoidal function, we assume that the rotary potential for $V_{pp} = 0$ V is also well approximated by the function. In fact, the experimental value [Fig. 4(b)] fits well with the theoretical result for a symmetric sinusoidal potential.

Next, we measured the mean square displacements (MSDs) [Fig. 3(a), right panel] defined as

$$\mathrm{MSD} = \langle [\theta(t+\Delta t) - \theta(t) - \langle \theta(t+\Delta t) - \theta(t) \rangle]^2 \rangle. \quad (6)$$

Then, using the MSD, we finally obtained the diffusion coefficients $D(N_{ex})$ of the rotary probe, defined as

$$D(N_{ex}) = \lim_{\Delta t \to \infty} \frac{\mathrm{MSD}}{2\Delta t}. \quad (7)$$

In Fig. 4(a), the dimensionless expression of the diffusion coefficient $D(N_{ex})\Gamma/k_BT$ is plotted as a function of N_{ex}/N_{max}, where N_{max} is the external torque value at which $D(N_{ex})$ has a maximum (this dimensionless expression was used to compare the result with the theoretical prediction [1]). Here, the value of the friction coefficient Γ of the bead duplex is estimated to be 1.1 pN nm s from the torque calibration experiment at $V_{pp} = 10$ V using beads (Sec. III in the Supplemental Material [11]), and T is 25 °C. We can see a clear peak in Fig. 4(a), while

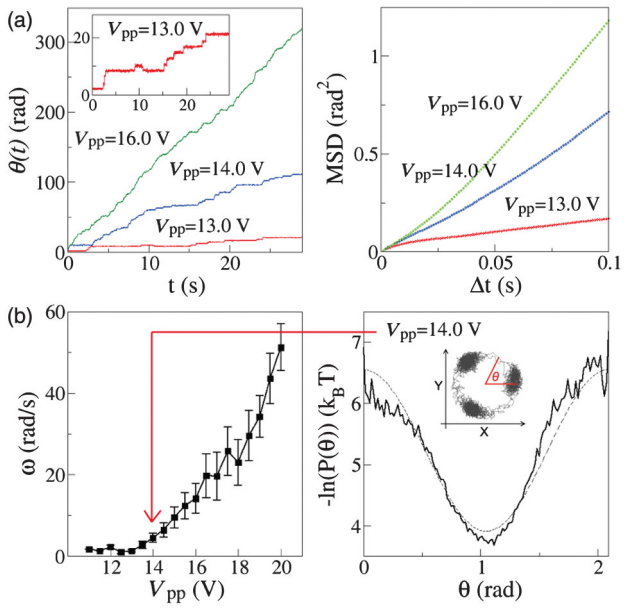

FIG. 3 (color). (a) Sample trajectories of a rotary angle $\theta(t)$ (left panel) and the MSD defined in Eq. (6) (right panel) for $V_{pp} = 13.0$, 14.0, and 16.0 V for the same F_1. By fitting the MSD with the linear function $ax + b$ in the range $0.05\ \mathrm{s} \le \Delta t \le 0.1$ s, we obtained the slope a. Then, D was calculated as $a/2$. (Inset) Enlarged graph of $\theta(t)$ for $V_{pp} = 13.0$ V. (b) Mean angular velocity ω (left panel), and plot of $-\ln[P(\theta)]$ (right panel) calculated for $V_{pp} = 14.0$ V, where $P(\theta)$ is the steady state distribution of θ. Error bars are statistical errors (left panel), and the dotted line denotes $1.3\cos(2\pi x/\ell) + 5.2$ (right panel). (Inset) Trajectory of bead duplex attached to F_1, plotted in the xy plane.

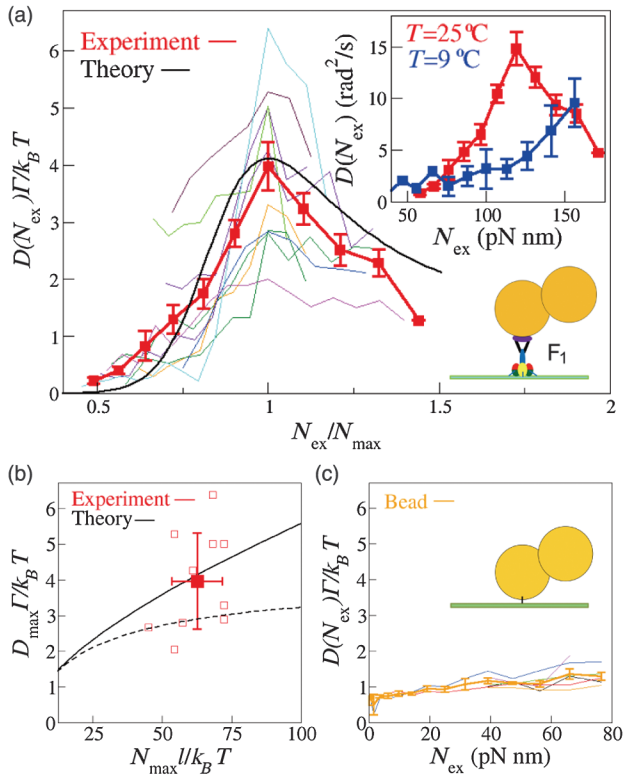

FIG. 4 (color). (a) $D(N_{ex})\Gamma/k_BT$ for ten different F_1 molecules as a function of N_{ex}/N_{max}. Here N_{max} is the torque at which $D(N_{ex})$ reaches its peak. The colors represent different molecules and the thick red curve represents the average over ten molecules. Error bars are statistical errors. The black solid line is from Eq. (3), by replacing x and f with θ and N_{ex}, for the sinusoidal potential [Eq. (4)] with $\Delta_E = 20k_BT$. (Inset) $D(N_{ex})$ vs N_{ex} for $T = 25\,°C$ (red line) and $T = 9\,°C$ (blue line). (b) $D_{max}\Gamma/k_BT$ as a function of $N_{max}\ell/k_BT$ for ten different F_1 molecules (the open red squares). The filled red square denotes the average. The error bars indicate the standard deviation. The black solid curve (dotted curve) is calculated based on Eq. (3) for a sinusoidal [Eq. (4)] [triangle (Eq. (5))] potential. (c) $D(N_{ex})\Gamma/k_BT$ as a function of N_{ex} in the absence of F_1. The error bars denote statistical errors.

$D(N_{ex})\Gamma/k_BT$ is constant [theoretically, $D(N_{ex})\Gamma/k_BT = 1$] in the absence of F_1 [Fig. 4(c)]. [The slight increase of $D(N_{ex})\Gamma/k_BT$ in Fig. 4(c) was discussed in Sec. III of the Supplemental Material [11].] The variation of $D(N_{ex})$ for F_1 can be seen in Fig. 4(a), which differs from the $D(N_{ex})$ obtained for beads without F_1 that is shown in Fig. 4(c). This variation may be due to a difference in the height and shape of the F_1 energy landscape. The possibility exists that the energy landscape of each F_1 protein was distorted in various ways by the applied torque since F_1 proteins have a plasticity. This type of intrinsic difference is sometimes observed in single-molecule experiments [17].

The energy barrier (Δ_E) in the case of [ATP] = 0 mM and [ADP] = 0.5 mM is measured to be approximately $20k_BT$ at 25 °C, from the comparison with the theoretical curve (3) [Fig. 4(a)]. Note that the black curve in Fig. 4(a) is obtained by replacing x and f with θ and N_{ex} in Eqs. (3) and (4). In Fig. 4(b), $D_{max}\Gamma/k_BT$ is plotted as a function of $N_{max}\ell/k_BT$, where ℓ ($= 120° = 2.1$ rad) is the period of the rotary potential of F_1. Indeed, the theoretical curve for the sinusoidal potential [Eq. (4)] is closer to the experimental result than that for the triangle potential [Eq. (5)].

Finally, we decreased the environmental temperature (to approximately 9 °C) using the fluid flow chip apparatus [18] (Sec. IV in the Supplemental Material [11]). The dwell times were increased at 9 °C (Fig. S4 of the Supplemental Material [11]). This implies that the energy barrier of the rotary potential of F_1 was increased. In the presence of ATP, it is known that the detachment of ADP from the F_1 catalytic site as an elementary step of ATP hydrolysis is decelerated dramatically at 9 °C due to the temperature-sensitive reaction [19,20]. Therefore, our observations under the condition ([ATP] = 0 mM, [ADP] = 0.5 mM) were also thought to be related to this phenomenon. Because the energy barrier of the ADP detachment at 9 °C became higher than that obtained at 25 °C, the peak in $D(N_{ex})$ at 9 °C could not be observed for $V_{pp} \leq 20$ V [Fig. 4(a), inset]. Further, the angular velocity [$\omega(N_{ex})$] at 9 °C was smaller than that obtained at 25 °C (Fig. S1 of the Supplemental Material [11]).

Summary.—In this paper, we observed the GA of diffusion for a tilted periodic potential, which was reported in Refs. [1–3] and which has not yet been demonstrated in biophysical application, in a single-molecule experiment on the rotary motor protein F_1-ATPase (F_1). As diffusion phenomena are universal, we believe that the methodology presented here is applicable to many physical systems.

This work was supported by Grants-in-Aid for Scientific Research to K. H. from the Ministry of Education, Culture, Sports, Science, and Technology (Japan) (MEXT) (Grants No. 23107703 and No. 26104501). We thank the members of the A. Ishijima and S. Takahashi laboratories for their helpful discussions, and Dr. S. Enoki, Dr. M. Tanigawara, and Dr. M. K. Sato for their assistance with the technical details of the experiments.

*kumiko@camp.apph.tohoku.ac.jp

[1] P. Reimann, C. Vanden Broeck, H. Linke, P. Hänggi, J. M. Rubi, and A. Pérez-Madrid, Phys. Rev. Lett. **87**, 010602 (2001).
[2] P. Reimann, C. Vanden Broeck, H. Linke, P. Hänggi, J. M. Rubi, and A. Pérez-Madrid, Phys. Rev. E **65**, 031104 (2002).
[3] G. Costantini and F. Marchesoni, Europhys. Lett. **48**, 491 (1999).
[4] S. Albaladejo, M. I. Marqués, F. Scheffold, and J. J. Sáenz, Nano Lett. **9**, 3527 (2009).
[5] S. H. Lee and D. G. Grier, Phys. Rev. Lett. **96**, 190601 (2006).
[6] M. Evstigneev, O. Zvyagolskaya, S. Bleil, R. Eichhorn, C. Bechinger, and P. Reimann, Phys. Rev. E **77**, 041107 (2008).

[7] P. Reimann and R. Eichhorn, Phys. Rev. Lett. **101**, 180601 (2008).
[8] D. Okuno, R. Iino, and H. Noji, J. Biochem. **149**, 655 (2011).
[9] E. I. Sunamura, H. Konno, M. Imashimizu-Kobayashi, Y. Sugano, and T. Hisabori, Plant Cell Physiol. **51**, 855 (2010).
[10] K. Hayashi and S. I. Sasa, Phys. Rev. E **69**, 066119 (2004).
[11] See Supplemental Material at http://link.aps.org/supplemental/10.1103/PhysRevLett.114.248101 for the experimental method and the low temperature experiments.
[12] J. Howard, *Mechanics of Motor Proteins and the Cytoskeleton* (Sinauer Associates, Sunderland, MA, 2001).
[13] V. Blickle, T. Speck, U. Seifert, and C. Bechinger, Phys. Rev. E **75**, 060101(R) (2007).
[14] H. Noji, R. Yasuda, M. Yoshida, and K. Kinosita, Jr., Nature (London) **386**, 299 (1997).
[15] R. Yasuda, H. Noji, M. Yoshida, K. Kinosita, Jr., and H. Itoh, Nature (London) **410**, 898 (2001).
[16] T. Watanabe-Nakayama, S. Toyabe, S. Kudo, S. Sugiyama, M. Yoshida, and E. Muneyuki, Biochem. Biophys. Res. Commun. **366**, 951 (2008).
[17] K. Hayashi, S. de Lorenzo, M. Manosas, J. M. Huguet, and F. Ritort, Phys. Rev. X **2**, 031012 (2012).
[18] Y. Inoue, M. A. B. Maker, H. Fukuoka, H. Takahashi, R. M. Berry, and A. Ishijima, Biophys. J. **105**, 2801 (2013).
[19] R. Watanabe, R. Iino, K. Shimabukuro, M. Yoshida, and H. Noji, EMBO Rep. **9**, 84 (2008).
[20] S. Enoki, R. Watanabe, R. Iino, and H. Noji, J. Biol. Chem. **284**, 23169 (2009).